Dynamic Vehicle Loading on a Slab Bridge Using Multiple Actuators

PAUL N. ROSCHKE

An analytical method is presented that approximates passage along a bridge deck of discrete wheel loads by a group of actuators. Actuators are fixed in position but controlled in a sequential manner according to a mathematical algorithm developed from a flexibility matrix approach. As an example, a large-scale laboratory model of a posttensioned flat slab bridge is loaded by an array of four actuators that simulates dynamic movement of a heavy truck. A total of 200,000 cycles of service load is applied to the slab in a region where transverse posttensioning forces impose high gradients of stress. Experimental readings from the laboratory are compared with predictions from numerical simulation. The algorithm can be applied to other types of bridge structures that undergo dynamic traffic loads.

Transportation-related structures are, by nature, subjected to live loads that move in a continuous fashion from one end of the structure to the other. Stress waves from these loads in the structural members are dynamic rather than static. Expensive maintenance of bridge decks and fatigue of related members attest to the importance of loads of this type.

In most studies of bridges that involve moving traffic, a cyclic concentrated load at a fixed location is used to approximate stresses from the vehicle. By contrast, Perdikaris et al. (*1*) used a moving wheel load and found that the fixed location method results in higher fatigue strengths at a higher number of stress cycles for concrete bridge decks. A variation on the fixed location method utilizes a moving single concentrated load that moves in a stepwise manner. In this case failure strength is lower than that for the fixed location method and occurs at fewer cycles (*2*).

For the current study, multiple fixed-load locations are used to represent effects of passage of wheel loads from a vehicle (see Figure 1). Two lines of loads, one for each wheelpath, are applied by means of a spreader bar at each actuator. The number of load locations is limited only by the number of available actuators. A time-varying load is applied by a controller at each actuator. By correct sequencing of loads applied by the actuators, dynamic effects caused by high-speed passage of a vehicle can be closely approximated. Also, front and rear wheel interaction is included in the stress wave patterns.

ALGORITHM FOR LOADING

Consider a structure such as a flat plate that is loaded by a vehicle moving along a given path. To obtain the pseudostatic load-deflection relations, a flexibility approach can be used. The basic equation of flexibility is

$$P \times f = u \tag{1}$$

Department of Civil Engineering, Texas Transportation Institute, Texas A&M University, College Station, Tex. 77843-3136.

where

P = applied load at a specified location j on a structure,
f = deflection or flexibility coefficient at any location i caused by a unit load applied at j, and
u = deflection at i caused by the load P.

Using superposition this relation may be expanded to include n load locations as follows:

$$\sum_{j=1}^{n} P_j f_{ij} = u_i \tag{2}$$

As an example, four actuators that have a fixed location are used in this study to apply simulated wheel loads at the eight locations indicated in Figure 1. In this case four flexibility equations may be written that relate the combination of the actuator forces to the deflection at four points in the slab. Here, the deflections of interest are taken to be at the actuator locations themselves. The equations are written for application of forces that cause the same deflection at these locations as a vehicle that is at an arbitrary location along its path of travel. Dividing the load applied by an actuator into two equal loads (two wheels per axle) results in the following equation for the average deflection under actuator 1:

$$\sum_{j=1}^{4} A_j (f_{1jPa} + f_{1jb}) = (u_{1a} + u_{1b}) \tag{3}$$

where

A_j = load applied by actuator j, assuming $A_j/2 = A_{ja} = A_{jb}$ with A_{ja} and A_{jb} being the loads that are transferred to the slab at actuator j;
f_{1ja} = flexibility coefficient for left actuator load (left and right defined by looking in the direction of traffic);
f_{1jb} = flexibility coefficient for right actuator load;
u_{1a} = deflection of slab at actuator 1 for left load; and
u_{1b} = deflection of slab at actuator 1 for right load. A similar equation may be written for the other actuators. For the case of four actuators, the equations are given in Equation 4.

$$\begin{bmatrix} (f_{11a}+f_{11b}) & (f_{12a}+f_{12b}) & (f_{13a}+f_{13b}) & (f_{14a}+f_{14b}) \\ (f_{21a}+f_{21b}) & (f_{22a}+f_{22b}) & (f_{23a}+f_{23b}) & (f_{24a}+f_{24b}) \\ (f_{31a}+f_{31b}) & (f_{32a}+f_{32b}) & (f_{33a}+f_{33b}) & (f_{34a}+f_{34b}) \\ (f_{41a}+f_{41b}) & (f_{42a}+f_{42b}) & (f_{43a}+f_{43b}) & (f_{44a}+f_{44b}) \end{bmatrix} \begin{Bmatrix} A_1 \\ A_2 \\ A_3 \\ A_4 \end{Bmatrix} = \begin{Bmatrix} u_{1a}+u_{1b} \\ u_{2a}+u_{2b} \\ u_{3a}+u_{3b} \\ u_{4a}+u_{4b} \end{Bmatrix} \tag{4}$$

In an analogous manner, a set of equations may also be written that relate wheel loads from a vehicle to the deflection at each actuator location. For a vehicle that has two wheels attached to each of three axles the equations are as follows:

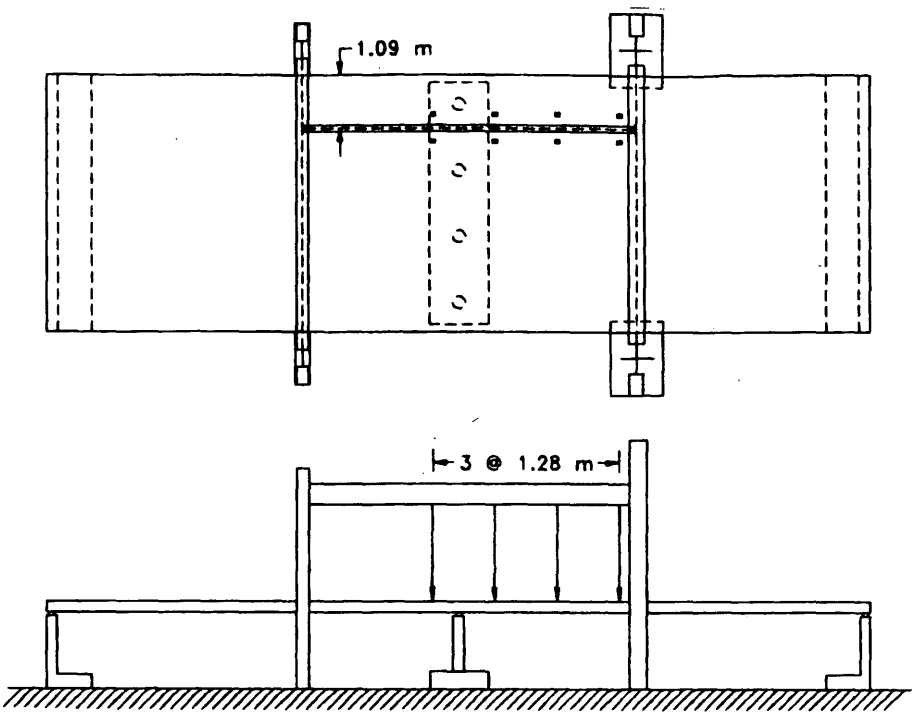

FIGURE 1 Fixed actuator locations for simulation of moving load.

$$\begin{bmatrix} (f^*_{11a}+f^*_{11b}) & (f^*_{12a}+f^*_{12b}) & (f^*_{13a}+f^*_{13b}) \\ (f^*_{21a}+f^*_{21b}) & (f^*_{22a}+f^*_{22b}) & (f^*_{23a}+f^*_{23b}) \\ (f^*_{31a}+f^*_{31b}) & (f^*_{32a}+f^*_{32b}) & (f^*_{33a}+f^*_{33b}) \\ (f^*_{41a}+f^*_{41b}) & (f^*_{42a}+f^*_{42b}) & (f^*_{43a}+f^*_{43b}) \end{bmatrix} \begin{Bmatrix} P_1 \\ P_2 \\ P_3 \end{Bmatrix} = \begin{Bmatrix} u_{1a}+u_{1b} \\ u_{2a}+u_{2b} \\ u_{3a}+u_{3b} \\ u_{4a}+u_{4b} \end{Bmatrix} \quad (5)$$

where

P_j = axle load;
f^*_{ija} = flexibility coefficient at the actuator for the left wheel load; and
f^*_{ijb} = flexibility coefficient at the actuator for the right wheel load.

As mentioned earlier, this set of pseudo-static equations holds for a given position of the moving vehicle.

Applying the condition at time t that deflections caused by the actuators (right side of Equation 4) be equivalent to those caused by the truck loads (right side of Equation 5), leads to the following relationship:

$$[f]\{A\} = [f^*]\{P\} \quad (6)$$

where matrixes f, f^*, A, and P are defined in Equations 4 and 5. Equation 6 can be solved for the required actuator forces for each position of the moving vehicle as it traverses the bridge.

EXAMPLE OF A SLAB BRIDGE

Recently, a 3/10-scale model of a two-span bidirectionally post-tensioned flat slab bridge (see Figure 2) was constructed and tested in a controlled laboratory environment (*3*). Dimensions of the slab are 16.9 × 5.33 × 0.229 m (55.5 ft × 17.5 ft × 9 in.). In addition to uniformly distributed longitudinal posttensioning, a band of tendons is placed in a narrow region above the four supporting columns. The slab rests directly on neoprene bearing pads that surmount the abutments and columns. No reinforcing steel connects the columns and abutments with the slab. Arrays of 185 strain gauges (see Figure 3), 18 linear variable differential transformers (LVDTs), 10 load cells, and 27 survey points serve to gather data for dead, live, and time-dependent loads.

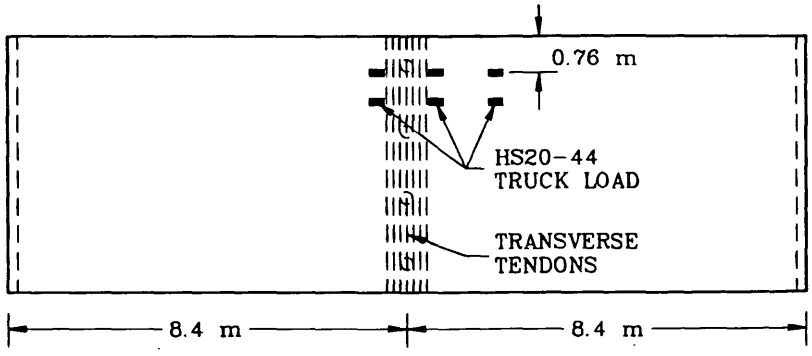

FIGURE 2 Slab geometry and example truck wheel load.

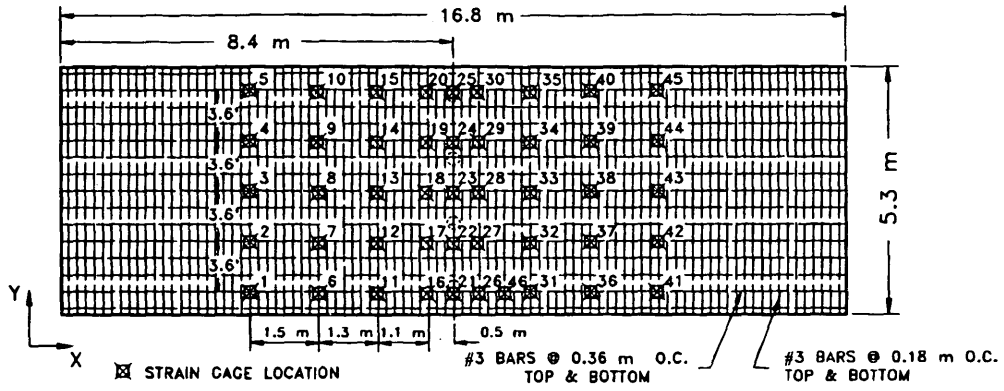

FIGURE 3 Location of strain gauges.

Factored and Scaled Truck Loads

Spacing and magnitude of the wheel loads on the laboratory model are determined by applying geometric and loading scale factors, along with impact and overload factors, to dimensions and load magnitudes of an AASHTO HS20-44 truck (see Figure 4). An impact factor of 0.30 is determined according to the following equation from AASHTO 3.8.2.1 (*4*):

$$I = \frac{50}{L_n + 125} \leq 0.3 \tag{7}$$

where

I = impact fraction (maximum 30 percent); and
L_n = length in feet of the portion of the span that is loaded to produce the maximum stress [for L_n = 8.38 m (27.5 ft) and I = 0.32, use 0.30].

Because design of the slab has been shown to be conservative (*3*), an overload factor of 1.67 (*4*) is also applied to increase the probability of inducing damage in the structure. The resulting wheel loads are multiplied by a similitude scale factor of 0.09 (*3*) to produce the wheel loads that are applied to the scale model bridge slab.

A region of the slab near the columns that has a high spatial gradient of stress was investigated for effects of repeated passage of heavy truck traffic. Traffic is assumed to flow across the bridge from right to left in Figures 1 through 3. Figure 2 shows a typical location of the truck tires along its path of travel. A beam attached to each actuator with a pin connection is used to transfer the load to pressure pads that are spaced equidistant from the center of the line of travel of the truck. These pads, which have the scaled dimensions of the area of contact of a truck tire, apply load to the bridge deck. The distance between actuators is equal to that of the scaled length of the wheelbase of the truck loading. This means that the actuator loads correspond to the given scaled truck loads at those instances in the loading cycle when the location of the simulated truck coincides with the pressure pads.

A preliminary static finite element analysis of the prestressed slab was carried out using TEXSLAB (*5*). The surface plot of Figure 5 shows the predicted normal stress in the transverse direction in the bottom layer of the slab as a result of prestressing and dead load. Figure 6 displays change in transverse stresses in the same bottom layer caused by the factored and scaled HS20-44 live load. Although stress ranges caused by live load are small, that is, approximately 345 kPa (50 psi), and a fatigue failure was not expected, it is still uncertain what damage might occur from the complex nature of the stress distribution in this region. Banding of transverse prestressing coupled with localized effects of column reactions may lead to a significant amount of microcracking when repeated loads are applied. To investigate this problem, 200,000 cycles of load are applied to the model.

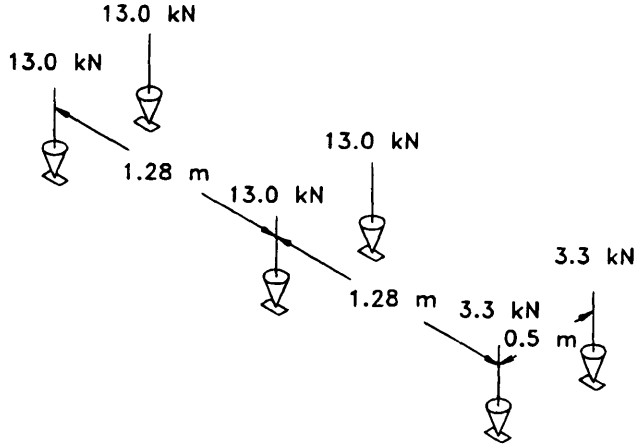

FIGURE 4 Wheel loads applied to scale model bridge slab.

Time History of Actuator Loading

Flexibility coefficients for Equation 6 are determined using the special-purpose finite element code mentioned earlier. A series of numerical simulations are carried out where the location of a unit load is varied by 0.61-m (2-ft) increments, beginning at the right end of the bridge deck. The load is placed in line with one of the paths of travel of a wheel (i.e., in line with the actuator pads), and deflection at each actuator pad is calculated. This gives one-half of the flexibility coefficients of Equation 6 for a given position of the load. A similar procedure is carried out for the other wheelpath. Then, knowing the flexibility coefficients and the magnitude of the truck wheel loads P_i (see Figure 4), leads to a simple solution for the actuator forces A_i that produce the same deflections at the actuators as the scaled vehicle.

Response time and mechanical constraints of the load actuators determine the maximum speed of load application for a single pas-

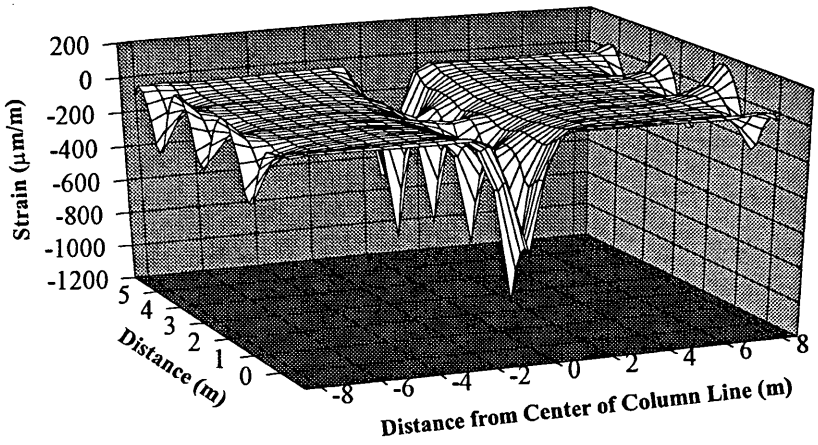

FIGURE 5 Transverse normal stress caused by dead load and prestressing.

sage of a vehicle. Because of hardware limitations of available actuators and their controllers, one full load cycle of travel may be applied in 1.66 sec. By applying a scale factor for velocity, it is determined that this corresponds to a truck traveling on the prototype bridge at 48 km/hr (30 mph). Correlation of time with truck position on the experimental slab gives a time history load curve for each actuator as shown in Figure 7*a*.

Two modifications of this procedure are made. Note that some negative (upward) values of load result as the actuators attempt to create the complex curvature of the structure. Because the lack of connectors on the surface of the experimental slab preclude tensile loads being applied by the actuators, a further approximation must be incurred. Equation 6 is solved by a trial-and-error procedure for each truck location with only one, two, or three actuators applying load. The combinations that result in no tensile load are used to create the necessary deflections.

Second, from Figure 7*a* the load from Actuator 4 becomes very high after the vehicle moves beyond the line of columns. This increase is because the fourth actuator is applying nearly all of the load to achieve the required deflection after the truck has passed this point. To reduce the influence of this actuator on the solution, the truck load is reduced to 0 after it moves past the center bent. The load curve that results from these special conditions is shown in Figure 7b.

Experimental Results

Consider a point on the slab that is 6.4 m (21 ft) from the beginning of the bridge and lies along a line that bisects the two lines of wheel loads. At this location, vertical displacement predicted by numerical simulation of the pseudostatic progression of the load is shown in Figure 8. Also shown in this plot is the actual displacement recorded by an LVDT from one cycle of the actuator loading. Differences between the curves are attributed to interaction of the dynamic response of the slab with the loads applied by the actuators. At the expense of rapid completion of the load cycles, the curve could be smoothed out with a slower application of the load. However, from the standpoint of fatigue, the additional spikes represent a more severe case of stress in the continuum than does a smooth curve.

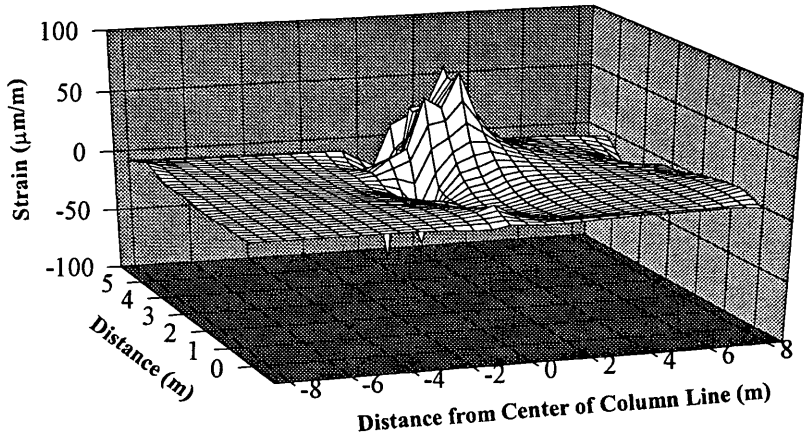

FIGURE 6 Change in transverse normal stress caused by live load.

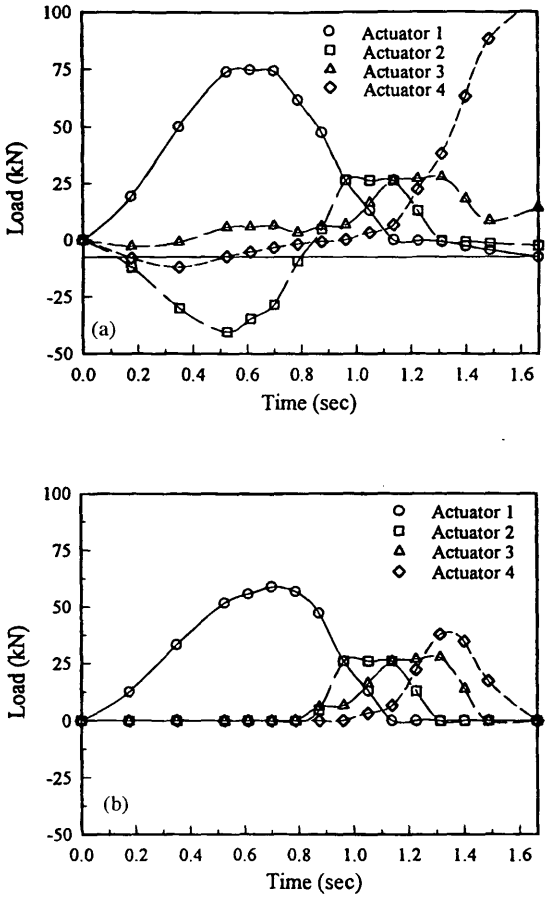

FIGURE 7 Load curves for application of cyclical load: (*a*) tensive forces allowed; (*b*) no tensile forces.

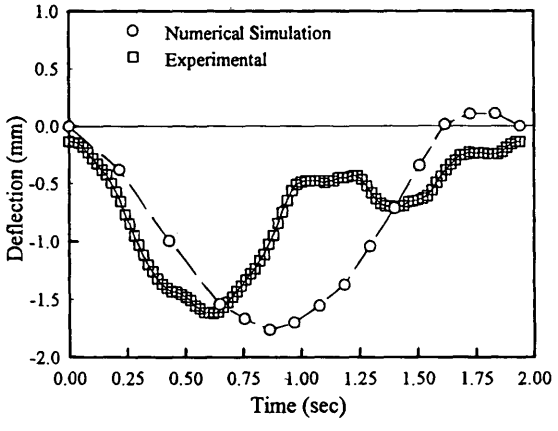

FIGURE 8 Comparison of experimental and theoretical deflection for one truck passage.

As described earlier, a total of 200,000 cycles of the HS20-44 truck was applied to the slab. Figure 9 shows a comparison of the initial deflection curve and one recorded during the last cycle at the same location as that described earlier. There are only small changes in the general shape and maximum deflection of the curves.

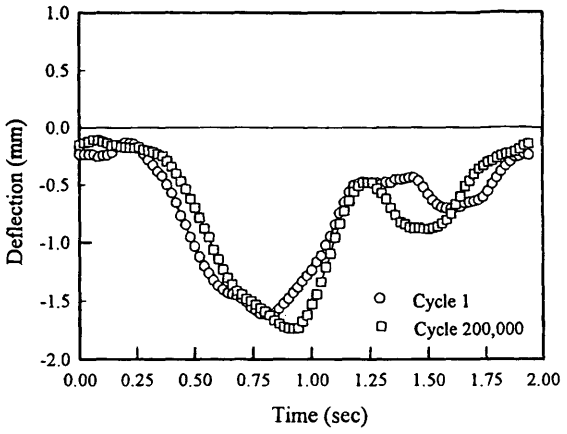

FIGURE 9 Comparison of deflection at first and last cycles.

Approximately once every 10,000 cycles, the dynamic loading was temporarily halted. A static load that is equivalent to the scaled and factored wheel loads was placed on the slab at the location shown in Figure 4. An LVDT located beneath the slab measured the deflection. For these static loads the measured deflection versus the number of load cycles is shown in Figure 10. During the first 20,000 cycles there is a decrease in vertical deflection resulting from the static load; this phenomenon is attributed to shifting of the structure and residual compression of the elastomeric bearing pads between the column and the slab. For the remaining 180,000 cycles the static deflection is relatively constant.

In addition to checking for change in vertical displacement at regular intervals of loading, attempts were also made to detect degradation of the concrete and to measure the change in transverse strain in the critical region near the columns. Cracking of concrete was monitored directly by visual inspection during application of the static load and, indirectly, by strain gauge readings. No visible cracks were observed on the top or bottom surface of the slab through the full number of cyclical loads. This lack of damage was confirmed by readings from the gauges attached to the rebars and embedded in the concrete (see Figure 3). Gauges located in the vicinity of the supporting columns recorded a change in strain of less than 5 microstrain for the static application of load. These negligible readings did not increase throughout the 200,000 cycles.

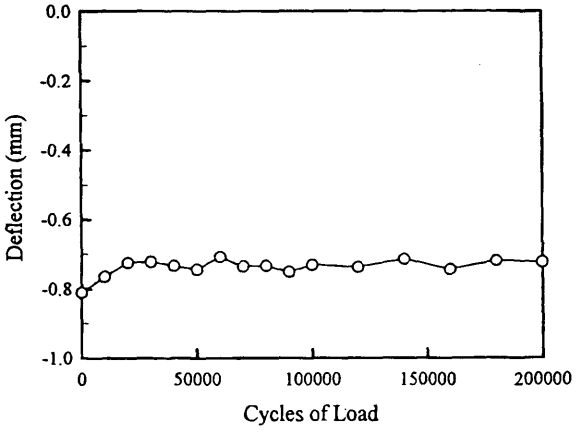

FIGURE 10 Static deflection versus cycles of load.

CONCLUSION

A method is presented that allows use of a series of actuators that are fixed in position to impose sequential loads that simulate passage of a vehicle along a bridge. The approach is demonstrated using a large-scale laboratory model of a slab bridge. Force time–history of each actuator is calculated from a system of simultaneous equations that govern each increment of time. Flexibility coefficients are determined from a static finite element analysis of the slab. Repetitive truck loading consisting of 200,000 cycles was applied to the slab at 2-sec intervals. Visual inspection and data from transducers show that no apparent damage to the concrete was sustained. Bidirectional posttensioning contributes to a conservative design of the slab that is not susceptible to fatigue damage at these load levels.

ACKNOWLEDGMENT

The author thanks the Texas Department of Transportation and FHWA for financial support for the study. VSL supplied post-tensioning equipment free of charge.

REFERENCES

1. Perdikaris, P. C., S. R. Beim, and S. N. Bousias. Slab Continuity Effect on Ultimate and Fatigue Strength of Reinforced Concrete Bridge Deck Models. *ACI Structural Journal,* Vol. 86, No. 4, 1989, pp. 483–491.
2. Okada, K., H. Okamura, and K. Sonoda. Fatigue Failure Mechanism of Reinforced Concrete Bridge Deck Slabs. In *Transportation Research Record 664*, TRB, National Research Council, Washington, D.C., 1978, pp. 136–144.
3. Roschke, P. N., K. R. Pruski, and C. D. Smith. *Experimental and Analytical Study of a Two-Span Post-Tensioned Bridge Slab.* Report FHWA/TX-90/1182-2. Texas Transportation Institute, Texas A&M University, College Station, 1992.
4. *Standard Specifications for Highway Bridges*, 14th ed. AASHTO, Washington, D.C., 1989.
5. Roschke, P. N., and K. R. Pruski. *Graphically-Oriented Analysis of Post-Tensioned Slab Bridges on Microcomputers.* Report FHWA/TX-90/1182-4F. Texas Transportation Institute, Texas A&M University, College Station, 1994.

Publication of this paper sponsored by Committee on Dynamics and Field Testing of Bridges.